Materials Science-Poland, 40(2), 2022, pp. 257-269
http://www.materialsscience.pwr.wroc.pl/
DOI: 10.2478/msp-2022-0024

Evaluation of CO_2 adsorption capacity with a nano-CaO synthesized by chemical combustion/ball milling

Francisco Granados-Correa[1,*], Melania Jiménez-Reyes[1]

[1]Instituto Nacional de Investigaciones Nucleares, Departamento de Química, Carretera México-Toluca S/N, La Marquesa, Ocoyoacac, Estado de México C. P. 52750, México

The adsorption of CO_2 on a nano-calcium oxide (nano-CaO) adsorbent was investigated under different conditions of temperature and supply pressure, considering kinetic, isotherm, and thermodynamic parameters. CaO is a crystalline material with a high surface area and nanosized particles with high porosity, which showed rapid initial CO_2 adsorption rates in the moderate temperature range studied. The adsorption was well described by the pseudo-second-order and the intraparticle diffusion kinetic models. The Langmuir isotherm model fitted the experimental data well, indicating a monolayer-type process. The thermodynamic parameters revealed that the CO_2/nano-CaO adsorption was endothermic, not spontaneous, and proceeded via physical and chemical processes. The activation energy value confirmed that the mechanism involved is a chemical process. In addition, the nano-CaO adsorbent could be regenerated five times without any significant loss of performance or properties. All the obtained results reveal that this porous nanoadsorbent has huge potential to be applied for CO_2-capture technologies on a large scale.

Keywords: *nano-CaO adsorbent, CO_2 adsorption, kinetics, isotherm, thermodynamics*

1. Introduction

The accelerated increase in atmospheric CO_2 concentration due to use of energy resources, such as the combustion of fossil fuels, is a cause of climate change, a vital global problem [1]. Thus, large-scale mitigation of CO_2 emissions represents an urgent need; great efforts have been made to develop novel CO_2-capture technologies considering efficiency, reductions in operating and maintenance costs, and retrofitting of power plants, among other characteristics [2]. Amine solvent adsorption, cryogenic methods, adsorption processes over solid adsorbents, and separation with porous membranes [3–6] are among the proposed methods that offer economic and environmental advantages; however, some of them have several important drawbacks in their use and application on a large scale [7].

CO_2 capture by adsorption in solid adsorbents is widely recognized as one of the most promising technologies to be used on a large scale, due to several factors, including its low operating costs and ease of application [8]. With this emphasis, great attention has been directed to the generation of highly promising adsorbents with improved properties to efficiently capture CO_2, such as activated carbons, zeolites, metal–organic frameworks, and metal oxides, among others [9]. Metal oxides have received particular attention, and it is important to note that calcium oxide (CaO) has been regarded as the most promising candidate for CO_2 capture, particularly structured as CaO nanoadsorbents [10–15], due to its long durability, good mechanical strength, high reactivity with CO_2, and low costs; indeed, it can be obtained from several sources and using various methods [16–18]. However, more research is needed before the CaO-based adsorbent can be placed in large-scale industrial use.

To improve CaO stability and functionality for CO_2 capture, different strategies have been examined [19]. One of them is the reduction of the particle size to the nanometer scale (<100 nm), looking for higher contact and reaction efficiencies; for this goal, mechanical milling is quite useful [20]. Data about the use of CaO adsorbents for CO_2 under typical flue gas conditions are limited

* E-mail: francisco.granados@inin.gob.mx

© Granados-Correa and Jiménez-Reyes 2022. This is an open access article distributed under the Creative Commons Attribution-NonCommercial-NoDerivatives 4.0 License. (http://creativecommons.org/licenses/by-nc-nd/4.0/)

[21, 22]. However, based on a theoretical calculation, Rashidi et al. [23] reported than 1 g of CaO can capture 786 mg of CO_2, whereas activated carbon typically captures 80 mg of CO_2/g. In this regard, CaO-based adsorbents are suitable materials to guarantee the industrial competitiveness of CO_2-capture technology and environmental applications at a relatively low cost. In a recent study [21], a novel porous nano-CaO adsorbent obtained by chemical combustion and ball milling was reported. This fast synthesis yielded interesting results because the ball milling treatment led to a high surface area, a low average crystalline size, and thus to a nanostructured nature. Structural and textural characteristics of these CaO nanoparticles indicated that they were highly reactive toward the adsorption of CO_2 molecules; therefore, interest remained about the influence of the adsorption parameters.

The main purpose of this study was to test the CO_2 adsorption behavior of the nano-CaO adsorbent, which was synthesized by the chemical combustion/ball milling method, and subjecting the adsorption process to different conditions. Kinetic, isotherm, and thermodynamic parameters were evaluated at moderate temperatures (25°C, 50°C, and 75°C) and supply pressures (1–15 atm). The properties of the nano-CaO adsorbent in terms of CO_2 desorption, stability, and regeneration ability were also analyzed. The study was focused to provide a better understanding of the adsorption mechanism and offer a useful approach to predict the adsorption behavior of this adsorbent.

2. Experimental

2.1. Reagents and materials

The analytical-grade reagents used for the chemical combustion synthesis of nano-CaO adsorbent were calcium nitrate tetrahydrate (Merck ACS, 98.0% purity) as the oxidizing agent and urea (Sigma Aldrich ACS, 99.9% purity) as the chemical fuel; these reagents were used without further purification.

2.2. Synthesis of the nano-CaO adsorbent

The nano-CaO adsorbent was prepared via a typical chemical combustion followed by a ball milling process [21]. The redox mixture contained urea as the chemical fuel and calcium nitrate tetrahydrate as the oxidizing agent, according to the following reaction:

$$2[Ca(NO_3)_2 \cdot 4H_2O]_{(s)} + 4CH_4N_2O_{(s)} + O_{2(g)} \rightarrow 2CaO_{(S)} + 16H_2O_{(g)} + 4CO_{2(g)} + 6N_{2(g)}$$

A 2:1 molar ratio of urea: calcium nitrate and a minimum volume of distilled water were thoroughly mixed in a porcelain crucible, so as to obtain a homogeneous mixture. This slurry was warmed to almost dryness and then 1 mL of distilled water was added. Finally, the resulting product was heated for 5 min at 800°C. The process was rich in fuel, which facilitated the formation of CaO because enough energy was available during combustion. The chemical combustion method has been traditionally used to prepare several metal oxides and other materials with fluffy structure, large surface areas, high porosity, and high yield [24]. The dried powders derived from the chemical combustion were subjected to mechanical ball milling for 2.5 h under argon atmosphere with a Spex-type mechanical ball mill, with stainless steel balls of 1 mm diameter, and a ball-to-powder weight ratio of 6:1. The dry ground CaO was the starting material for the study of CO_2 adsorption.

2.3. Adsorbent characterization

The CaO was characterized using the techniques described below.

(A) X-ray diffraction (XRD) analysis with a SIEMENS D-5000 powder diffractometer in a wide-angle region of 10°–100° in the 2θ scale, and the diffraction pattern was compared to the database in the International Centre for Diffraction Data, Pennsylvania, USA.

(B) Scanning electron microscopy (SEM) with electron diffraction scattering (EDS) analysis (JEOL JSM-5900LV with an Oxford

EDS microprocessor) for knowing the morphology of the CaO powders and their elemental semiquantitative composition.

(C) N_2 physisorption measurements were performed at −196°C (Belsorp Max Japan Inc. instrument), and the corresponding surface area was determined by the Brunauer-Emmett-Teller (BET) method of multiple points; the total pore volume (V_{Tp}), the mean pore radius (R_p), and the pore size distribution were derived using the Barrett-Joyner-Halenda (BJH) method. To obtain the greatest gas adsorption capacity and to release the water and impurities adsorbed, the CaO samples were degassed at 200°C for 3 h under a nitrogen atmosphere before measurements.

2.4. CO_2 adsorption kinetic experiments

Kinetic adsorption experiments of CO_2 onto the nano-CaO adsorbent were conducted at different temperatures (25°C, 50°C, and 75°C) and at room pressure using a 50 mL capacity Parr 4592 stainless steel pressure reactor coupled to a temperature-controlled system. Samples of 10 mg of the nano-CaO adsorbent were exposed to a high-purity (99.98%) dry CO_2 flow at 1 atm pressure for 1 min, 3 min, 5 min, 10 min, 15 min, 20 min, 25 min, 30 min, 45 min, 60 min, 90 min, and 180 min. Prior to the CO_2 adsorption tests, the adsorbent samples were degassed for 30 min under vacuum at 325°C to remove some possible impurities. Measurements of the CO_2 adsorption capacity were performed by thermogravimetric analysis (TGA) with a TGA analyzer (SDT Q600; TA Instruments) coupled with a mass spectrum analyzer (TA Instruments, LLC). For these analyses, the CaO sample (~6 mg) was put in a ceramic cell and then heated from 20°C to 850°C at the rate of 10°C/min, in an inert atmosphere of helium (100 mL/min). The quantity of CO_2 (millimoles) captured per gram of adsorbent (millimoles per gram [mmol/g]) was calculated from the TGA calcination profile for different contact times and temperatures based on the weight loss of CO_2; the first derivatives of the TGA curves (differential thermal analysis [DTA]) were also computed.

2.5. CO_2 adsorption isotherms

The adsorption isotherms of CO_2 in the porous nano-CaO adsorbent were determined at 25°C, 50°C, and 75°C and under different CO_2 gas pressures (1 atm, 5 atm, 10 atm, and 15 atm). The adsorption capacity of CO_2 was measured by TGA as for the kinetic tests. Classic Langmuir and Freundlich isotherm models were used to provide a mathematical description of the CO_2 adsorption process on the nano-CaO adsorbent, and their respective constants were determined. These isotherm models generally provide information on the CO_2 adsorption mechanisms and affinity properties of the adsorbents.

2.6. CO_2 adsorption thermodynamics

The effect of temperature on the amount of CO_2 adsorbed by the nano-CaO adsorbent was studied at 298 K, 323 K, and 348 K. The nano-CaO adsorbent dosage, the flow, and the CO_2 pressure were constant. The most important thermodynamic parameters, such as standard enthalpy (ΔH°), standard entropy (ΔS°), standard free energy (ΔG°), and activation energy (E_a), of CO_2 adsorption were determined.

2.7. Cyclic CO_2/nano-CaO adsorption-desorption

The CO_2 adsorption-desorption activity of the nano-CaO adsorbent was determined as follows. First, adsorption of CO_2 onto nano-CaO adsorbent was carried out at 75°C and 1 atm, and the adsorption capacity q_{ad} was measured in these conditions. Then, these CO_2/nano-CaO samples were exposed to a helium flow from 20°C to 850°C for eliminating CO_2. Thereafter, CO_2 was again adsorbed onto the same samples of the nano-CaO adsorbent. Five cycles of adsorption-desorption were achieved.

3. Results and discussion

3.1. Adsorbent characterization

The chemical combustion/ball milling method allowed the preparation of a large amount of voluminous, spongy, and nanocrystalline CaO adsorbent with a large surface area and high porosity.

Figure 1 shows the XRD pattern of the adsorbent, in which the CaO is the most important mineral component of the sample (International Centre for Diffraction Data, file: 37-1497). The crystallite size of the CaO particles using the Scherrer equation was 18.61 nm, showing a nanostructured material. In addition, a crystalline structure of $CaCO_3$ appears as a trace component (International Centre for Diffraction Data, file: 05-0586).

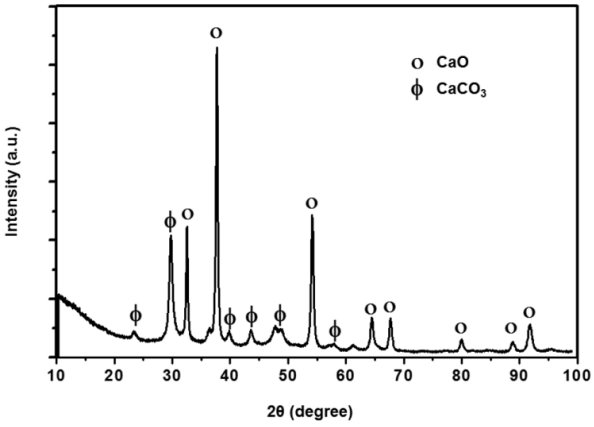


Fig. 1. XRD diffraction pattern of the nano-CaO adsorbent.
Note: XRD, X-ray diffraction

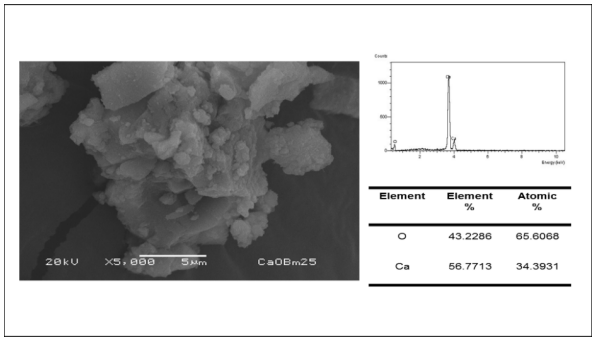


Fig. 2. SEM micrograph of Cao adsorbent at 5000× and EDS analysis.
Notes: EDS, electron diffraction scattering; SEM, scanning electron microscopy

The SEM micrograph of the CaO (Figure 2) adsorbent shows an agglomeration of nanoparticles with a well-developed and irregularly shaped porous structure, rough surface, and a small particle size (<10 μm) due to the fragmentation caused by the mechanical ball milling. In this regard, the agglomerates have substantial surface texture, porosity, and big surface area. A porous structure facilitates CO_2 access to the active sites and thereby increases the rates of CO_2 physisorption, chemisorption, and diffusion. The quantitative microanalysis of the nano-CaO adsorbent using SEM with X-ray energy dispersion only confirmed the presence of calcium and oxygen elements in this sample; a high CaO content in the adsorbent structure favors the conversion of CaO into $CaCO_3$.

N_2 physisorption at 77 K showed that the CaO adsorbent had a large BET surface area of 50.73 m^2/g (which is indicative of highly developed porosity), a high total pore volume of 0.548 cm^3/g, and a narrow and uniform size distribution of the pore radius, which was determined by the BJH method to be 19.24 nm with an ~80% distribution (Figure 3). These improved structural and textural properties all played an important role in capturing CO_2 and showed a high CO_2 adsorption performance of the adsorbent when it was exposed to a flow of CO_2 at different temperatures.

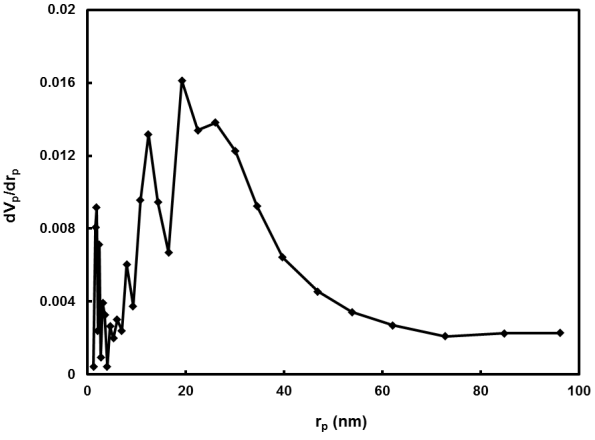


Fig. 3. Determination of pore-size distribution by the BJH method.
Notes: BJH, Barrett-Joyner-Halenda

3.2. CO_2 adsorption kinetics

The adsorption kinetics describes the adsorption rate of the adsorbate, which governs the residence time of the adsorption reaction. The rate at which adsorption occurs is therefore of paramount

Table 1. Kinetic parameters evaluated for the process of CO_2 adsorption onto the nano-CaO adsorbent at different temperatures

Models	**Parameters**	**Temperature**		
		25°C	**50°C**	**75°C**
Pseudo-first-order model	k_1 (/min)	0.24	0.58	0.13
	q_{max} (mmol/g)	4.59	3.81	5.27
	R^2	0.78	0.58	0.74
Pseudo-second-order model	k_2 (/min)	3.41	1.4	0.20
	q_{max} (mmol/g)	9.02	10.08	11.02
	R^2	0.9999	0.9996	0.9998
Elovich	α (mmol/g)	176.8	122.1	41.2
	β (mmol/g)	1.00	1.16	1.40
	R^2	0.48	0.50	0.59
Intraparticle diffusion	q_e (mmol/g)	7.56	8.33	8.53
Step 1 ($0 < t < 1$ min)	k_{ip1} (mmol/g min$^{1/2}$)	4.36	4.81	4.92
Step 2 ($1 < t < 10$ min)	R^2	0.87	0.85	0.90
	q_e (mmol/g)	3.38	3.51	4.64
	k_{ip2} (mmol/g min$^{1/2}$)	0.87	0.90	1.19
	R^2	0.995	0.94	0.94

importance in the design of an appropriate adsorption system, and thus, understanding the kinetics of adsorption is vital for capturing CO_2 because it provides essential information on the possible speed control steps (e.g., chemical reaction, diffusion control, and mass transfer) [25]. In the present study, kinetic models were used to investigate the CO_2 adsorption behavior on nano-CaO adsorbent under a range of temperatures and durations, ranging from 1 min to 180 min. The correlation coefficients (R^2) determined the conformity between the experimental data and each kinetic model, which were the pseudo-first-order [26], pseudo-second-order [27], Elovich [28], and intraparticle diffusion [29] models, the most widely used for describing adsorption processes. The results obtained are shown in Table 1.

Data of Table 1 show that the correlation coefficient (R^2) for the pseudo-second-order model is higher than for the other ones, which indicates that this model was the most appropriate for describing the kinetics of CO_2 adsorption onto the nano-CaO adsorbent. The corresponding equation is as follows (Figure 4):

$$\frac{t}{q_t} = \frac{1}{k_2 {q_e}^2} + \left(\frac{1}{q_e}\right) t, \tag{1}$$

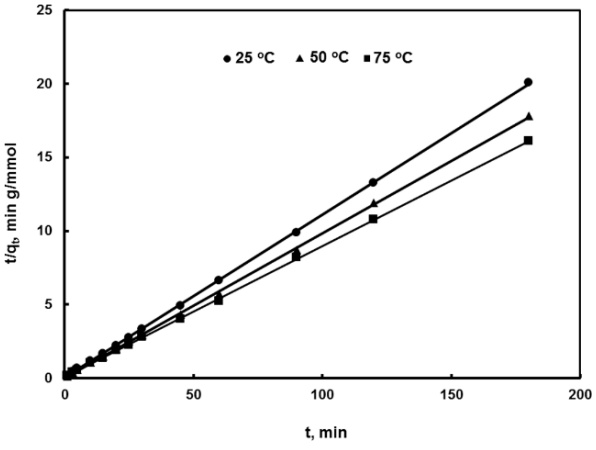


Fig. 4. Kinetic data of CaO adsorption onto nano-CaO adsorbent, at different temperatures and 1 atm pressure.
Notes: Linear plots of the pseudo-second-order model: t/q_t = 0.11t + 0.004 (25°C); t/q_t = 0.099t + 0.02 (50°C); t/q_t = 0.089t + 0.05 (75°C); R^2 = 0.9. q_t = the amount of CO_2 adsorbed at time t; R^2, correlation coefficient

where q_e and q_t are the amounts of CO_2 adsorbed (in mmol/g) at equilibrium and at time t (in minutes), respectively, and k_2 is the pseudo-second-order adsorption rate constant (/min). According to this model, it is assumed that the rate-limiting step can be chemisorption, which involves valence

forces through the sharing or exchange of electrons between adsorbate (gas molecules) and adsorbent [29]. Moreover, the occupation of the velocity adsorption sites is proportional to the number of unoccupied sites, and the adsorption site occupancy rate is proportional to the square of the number of unoccupied sites.

For the process CO_2/nano-CaO, the maximum adsorption capacity (q_e, mmol/g) increases with temperature (25°C, 50°C, and 75°C) at room pressure, whereas the rate constant diminishes with this parameter. This effect suggests a greater driving force of the gas molecules when temperature increases, leading to faster diffusion of CO_2 and an increase in CO_2 capture. These kinetic results are important regarding cost-effective adsorption technologies because the pollutant CO_2 is removed in a relatively short time. For all the studied conditions, CO_2 adsorption was observed in the first minute of contact, equilibrium was achieved in approximately 15 min, and no further changes in CO_2 adsorption were observed afterward. The increasing of CO_2 adsorption with the contact time prior to reaching equilibrium is due to the high availability of the active sites of the adsorbent, and the process slowed in the later stages of contact time due to a decrease in the number of active sites. The experiments for determining other adsorption parameters were carried out with 20 min contact time.

The values of R^2 for the intraparticle diffusion model are good enough as well. The equation of this model is the following:

$$q_t = K_{iP}\sqrt{t} + I, \tag{2}$$

where K_{iP} corresponds to the rate constant of each step of the process and I is the intercept that provides an idea about the boundary layer thickness: i.e., the larger the intercept, the greater is the boundary layer effect (in mmol/g). According to this model, the gas molecules may diffuse into the particles when the solid adsorbent is porous enough. The adsorption of the gaseous phase on and in the adsorbent may occur via three main stages: (1) transport of the gas molecules from the volumetric phase to the adsorbent surface; (2) diffusion of the gas molecules from the surface to the adsorbent pores; and (3) diffusion in the interior of the pores.

Data on the adsorption of CO_2 by the CaO nanoparticle adsorbent treated according to Eq. (2) showed that it was a multilinear process (Figure 5). The first line corresponds to the instant adsorption from the volumetric phase to the surface of the adsorbent; the second section is attributed to the gradual intraparticle diffusion; and the third line corresponds to the final equilibrium stage [25]. The first stage was very fast and was completed in the first 1 min; the second stage of intraparticle diffusion was reached at 10 min; thereafter, equilibrium was achieved. The value of K_{iP} for the first stage was higher than that of the second one (Table 1). Therefore, the adsorption of CO_2 on the highly porous nano-CaO adsorbent was probably not only due to intraparticle diffusion but this mechanism may be a consequence of the adsorption itself.

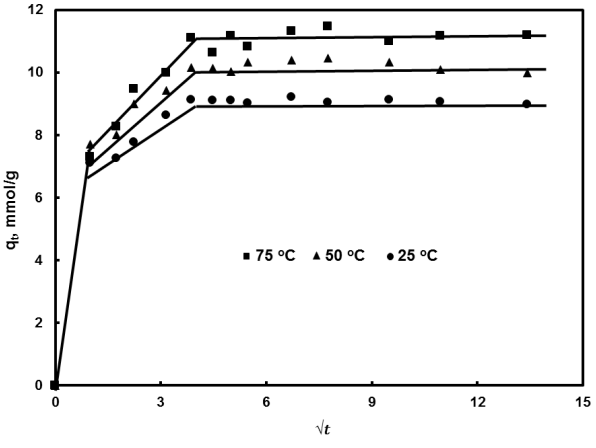


Fig. 5. Kinetic data of CaO adsorption onto nano-CaO adsorbent, at different temperatures under 1 atm pressure.
Notes: Linear plots correspond to the intraparticle diffusion kinetic model. (1) $q_t = 7.1\sqrt{t}$, $q_t = 0.73\sqrt{t}+6.2$ ($R^2 = 0.94$), and $q_e = 9.2$ (25°C). (2) $q_t = 7.7\sqrt{t}$, $q_t = 0.86\sqrt{t}+6.7$ ($R^2 = 0.96$), and $q_e = 10.3$ (50°C). (3) $q_t = 7.72\sqrt{t}$, $q_t = 0.86\sqrt{t}+6.7$ ($R^2 = 0.97$), and $q_e = 10.9$ (75°C). q_e, the amount of CO_2 adsorbed at equilibrium; q_t = the amount of CO_2 adsorbed at time t; R^2, correlation coefficient

Table 2. Summarized linear isotherm parameters for CO_2 adsorption on nano-CaO adsorbent at the temperatures of 25°C, 50°C, and 75°C and at pressures of 1 atm, 5 atm, 10 atm, and 15 atm for each temperature

Temperature (°C)	Langmuir constants			Freundlich constants		
	q_{max} (mmol/g)	K_L (/atm)	R^2	K_F (mmol/g [atm]$^{1/n}$)	1/n	R^2
25	10.74	0.48	0.996	0.111	0.049	0.78
50	11.31	0.35	0.998	0.099	0.022	0.75
75	12.55	0.31	0.998	0.091	0.009	0.88

3.3. CO_2 adsorption isotherms

Data of q_e obtained under different supply pressures (1 atm, 5 atm, 10 atm, and 15 atm) and at different temperatures (25°C, 50°C, and 75°C) were treated using the linear equations of both Langmuir [30] and Freundlich [31] adsorption isotherm models. The results are presented in Table 2, where the higher value of the correlation coefficient (R^2) corresponds to the Langmuir model. The linear form of this model is expressed as follows:

$$\frac{P_{CO_2}}{q_e} = \left(\frac{1}{q_{max}}\right) P_{CO_2} + \left(\frac{1}{K_L\, q_{max}}\right) \qquad (3)$$

where P_{CO2} is the pressure (in atmospheres) of the adsorbed gas CO_2, q_e is the adsorption capacity of CO_2 at equilibrium (mmol/g), q_e is the maximum adsorption capacity of CO_2 at equilibrium (mmol/g), and K_L (/atm) is the Langmuir isotherm constant, which represents the affinity between the adsorbent and adsorbate and may be used to predict whether an adsorption system is favorable or unfavorable.

The Langmuir isotherm parameters at 25°C, 50°C, and 75°C were evaluated from the slopes and the intersections of the plots P_{CO2}/q_e versus P_{CO2} (Figure 6). As expected, the CO_2 adsorption capacity increased with the CO_2 pressure, which is the driving force of the adsorption process. Based on the data of Table 2, both K_L and q_{max} increase with temperature. This indicates that the adsorbent surface was well coated with CO_2 molecules as a result of their higher surface affinity by implementing a chemisorption behavior. CO_2 must be chemisorbed on fixed surface sites.

Moreover, according to the Langmuir model, the surface of the porous nano-CaO adsorbent is homogeneous, and CO_2 adsorption occurs in a monolayer of CaO; in this case, the formation of multilayers, as proposed by the Freundlich model, is restricted [32].

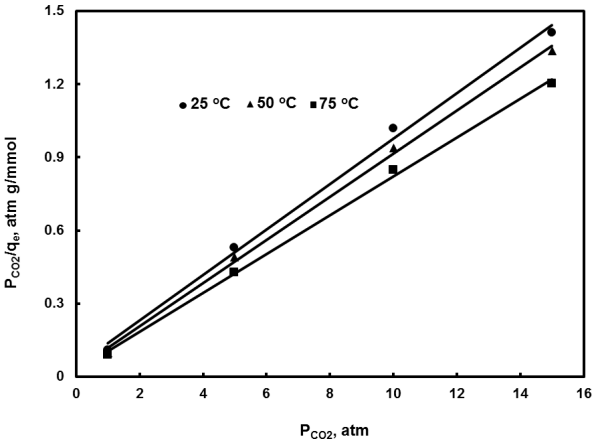


Fig. 6. Isotherm data of CaO adsorption onto nano-CaO adsorbent, at different temperatures.
Notes: Linear equations of the Langmuir model: (1) P_{CO2}/q_e = 0.093 P_{CO2} +0.045 (R^2 = 0.996) (25°C). (2) P_{CO2}/q_e = 0.088 P_{CO2} +0.031 (R^2 = 0.998) (50°C). (3) P_{CO2}/q_e = 0.080 P_{CO2} +0.024 (R^2 = 0.998) (75°C). P_{CO2}, pressure of the adsorbed gas CO_2; q_e is the maximum adsorption capacity of CO_2 at equilibrium; R^2, correlation coefficient

The essential characteristics of the Langmuir isotherm can be expressed in terms of a dimensionless constant called the separation factor (R_L), which examines the favorable acceptance of the adsorption process [33]. An adsorption process is irreversible if R_L =0, favorable if $0 < R_L < 1$, linear if R_L = 1, and unfavorable if $R_L > 1$. The equation for determining the dimensionless R_L values is the following:

$$R_L = \frac{1}{1 + K_L P_{CO2}} \qquad (4)$$

where K_L is the Langmuir constant or the affinity constant (/atm), and P_{CO2} is the equilibrium pres-

sure of the adsorbed gas (in atmospheres). From the experimental results, the R_L terms showed values from 0.67 to 0.12 (25°C), from 0.74 to 0.16 (50°C), and from 0.77 to 0.18 (75°C), for the range of pressure from 1 atm to 15 atm. These values of R_L, which are <1, indicate that the conditions of the adsorption process are favorable.

3.4. CO_2 adsorption thermodynamics

Important factors, such as energy changes in a reaction, should be considered when developing an adsorption system, and thermodynamic concepts are required to achieve this outcome. The thermodynamic parameters provide in-depth information on the inherent energy changes associated with adsorption mechanisms. To evaluate these parameters, the linearized form of the van't Hoff modified equation is the following:

$$\ln K_L = -\frac{\Delta H^0}{R}\left(\frac{1}{T}\right) + \frac{\Delta S^0}{R}, \tag{5}$$

where K_L is the Langmuir equilibrium constant; ΔH° and ΔS° are the enthalpy and entropy changes, T is the absolute temperature (in Kelvin), and R is the universal gas constant (8.314×10^{-3} kJ/mol K). The slope and intersection of the straight-line diagram of lnK_L versus $1/T$ allows the determination of the values of ΔH° and ΔS° (Figure 7).

The thermodynamic analysis revealed that the adsorption process is endothermic due to the positive value of ΔH° = 32.6 KJ/mol. The magnitude of ΔH° can also be used to distinguish between the mechanisms of physisorption (<20 kJ/mol) and chemisorption (~80 kJ/mol to 200 kJ/mol) [34]. As physisorption arises from relatively weak interactions, such as the van der Waals force, chemisorption involves stronger chemical interactions. According to Moroto-Valer et al. [35], the process of physisorption involves a high surface adsorption of energy and the diffusion of molecules at elevated temperatures. The ΔH° value obtained for CO_2 adsorption onto the CaO sample was 32.6 kJ/mol, which is indicative of both physisorption and chemisorption processes. The ΔS° value was 0.102 kJ/mol K, and the positive value reflects the affinity of CO_2 for the nano-CaO adsorbent and

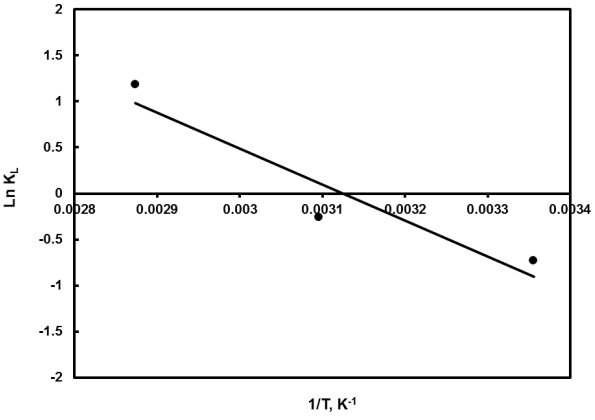


Fig. 7. Thermodynamic data of CaO adsorption onto nano-CaO adsorbent, at different temperatures under 1 atm pressure.
Notes: Linear plot of the van't Hoff modified equation: $\ln K_L = -3917\,(1/T) + 12.2$ ($R^2 = 0.9$). K_L, the Langmuir isotherm constant; R^2, correlation coefficient

suggests a high disorder of the adsorbate molecules during the fixation of the CO_2 molecules onto the active sites of CaO. According to Pighini et al. [36], entropy change is related to the mobility of CO_2 and to the coverage on the adsorbent; a high entropy value must be related to chemisorption.

The Gibbs free energy change (ΔG°) is an important criterion for spontaneity, and both energetic and entropy factors must be considered for its evaluation; according to the following equation:

$$\Delta G^\circ = \Delta H^\circ - T\Delta S^\circ. \tag{6}$$

The results of ΔG° were of a positive sign, which implies a nonspontaneous adsorption reaction [37]; moreover, these values diminish with temperature (3.2 KJ/mol, 1.7 KJ/mol, and 0.7 KJ/mol at 298 K, 232 K, and 348 K, respectively), which suggests that the adsorption of CO_2 on the CaO-based nanoadsorbent is more favored at higher temperatures.

The adsorption activation energy (E_a) was calculated by using the Arrhenius linear equation:

$$\ln k_v = \frac{E_a}{R}\left(\frac{1}{T}\right) + ln\,A \tag{7}$$

where k_v is the velocity constant, A is the independent temperature factor (millimoles of substrate

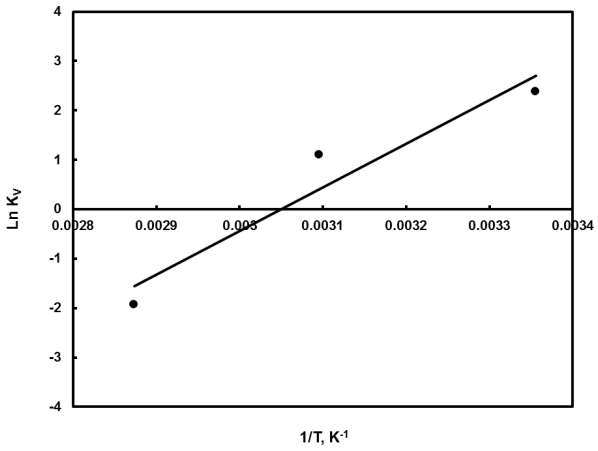


Fig. 8. Thermodynamic data of CaO adsorption onto nano-CaO adsorbent, at different temperatures under 1 atm pressure.
Notes: Linear plot of the Arrhenius equation: ln k_V = 8830 (1/T) – 26.9 (R^2 = 0.93). k_v, the velocity constant; R^2, correlation coefficient

per milligram per minute [mmol/mg min]), R is the universal gas constant (8.314 × 10^{-3} kJ/mol K), T is the temperature (in Kelvin), and E_a is the activation energy of adsorption (in kilojoules per mole [kJ/mol]). This is the minimum energy that must be overcome by the adsorbate molecules and it defines the velocity of the process [38].

The values of the velocity constants of the pseudo-second-order kinetic model at 298 K, 323 K, and 348 K (Table 1) were incorporated into Eq. (7) as a function of 1/T (Figure 8). The values of the slope and the ln k_V = 0 intersection of that plot allowed us to obtain E_a = −73.4 KJ/mol and ln A = ~26.9. Otherwise, considering the experimental data of k_V at 298 K and 348 K and the Arrhenius equation, in which the factor A is eliminated, we get the following expression:

$$ln\left(\frac{K_{v1}}{K_{v2}}\right) = -\frac{E_a}{R}\left(\frac{1}{T_1} - \frac{1}{T_2}\right) \quad (8)$$

The calculated value of E_a = −74.3 KJ/mol was virtually the same as that obtained from Eq. (7). The value of E_a (~80 KJ/mol) confirms that the adsorption mechanism is chemisorption. Typically, physisorption requires low E_a values, whereas chemisorption is characterized by higher values [39]. In general and based on the signs and magnitudes of the thermodynamic parameters obtained in the present study, it can be established that the adsorption of CO_2 on the porous nano-CaO adsorbent is mainly produced by chemical adsorption through a thermodynamically nonspontaneous process, and the adsorption of CO_2 molecules is positively temperature dependent. These data provide valuable information for the design of improved adsorption schemes to capture CO_2 using a new nanoadsorbent based on CaO.

3.5. Mechanism of CO_2 adsorption onto the nano-CaO adsorbent

CO_2 capture technologies require the understanding of the adsorption mechanism to enable use of an adsorbent at the industrial level. According to the literature, a gas-solid carbonation reaction occurs when CaO is directly combined with CO_2 [40]. In the CaO-CO_2 reaction, the CO_2 molecules can interact with the CaO surface, and when this occurs, carbonation directly follows. The chemical reaction may progress until the complete formation of the carbonate thin layer on the surface of the CaO particles, but this layer may block the access of CO_2 to the internal active CaO sites of the particles. For chemisorption, the CO_2 molecule must diffuse into the pores of the adsorbent and interact with the internal surface of the adsorbent [41]; it has also been shown that reducing the crystallinity of the adsorbent favors diffusion and promotes recharging [42].

In this study, the crystalline structure of the adsorbent, based on CaO, and both the particle and crystal sizes were reduced by the ball milling treatment. This caused a beneficial effect of more conversion from CaO to $CaCO_3$, attributed to the CaO nanoadsorbent's fluffy structure, significant surface area, and large pore volume, which allows CO_2 molecules to easily diffuse into the pore structure and reach deeper active sites, which leads to maximum CO_2 capture.

In this framework, the nanostructured nature of CaO caused reactivity and increased adsorption effects involving many active surface sites available for CO_2 adsorption. This also allowed the introduction of a large amount of CO_2 into its meso-

pores in a well-dispersed manner that favors the gas-solid diffusion reaction and results in increased CO_2 capture. As observed in our results, a mesoporous nano-CaO adsorbent, with a mean pore radius of 19.24 nm at approximately 80%, was obtained. In this way, we improved intraparticle diffusion in the CO_2 capture process in the porous CaO because the kinetic radius was sufficient for the diffusion of CO_2 molecules within the CaO porous structure when considering a CO_2 molecular size of 0.33 nm. The carbonation reaction in the micropores is hindered by a limited space that restricts the growth of $CaCO_3$. For CO_2 capture with CaO-based adsorbents, mesopores (2–50 nm in diameter) are expected to play an important role based on previous studies on carbonation. Furthermore, these pore types are the dominant contributors to the carbonation reaction and have a high surface area and high pore volume that accommodates the bulky $CaCO_3$ product [43]. The chemical adsorption for the whole process in this material has also been confirmed. Yet, to the best of our knowledge, the physical adsorption process is also controlled by the pore characteristics of the adsorbent, and the micropores (d_p <2 nm) create more selective CO_2 adsorption. According to Lee and Park [44], the gas adsorption potential reaches a maximum at the subnanometer scale, when the gas molecules begin to overlap with reducing pore size. This results in a much higher bonding energy emanating from the formation of deep potential fields from the neighboring walls, which leads to an increase in the surface area. In our case, narrow pores of the prepared nano-CaO adsorbent were approximately 15% of the total, which were also responsible for the physical capture of CO_2.

Finally, it is possible that the most appropriate reaction mechanism in this solid-gas system mainly occurred by chemisorption, with a carbonation reaction on the surface amid a favorable pore morphology of the CaO adsorbent obtained after treatment by ball milling. This was clearly verified by XRD, Fourier transform infrared spectroscopy (FTIR), and X-ray photoelectron spectroscopy (XPS) analysis. However, a very small fraction of physisorption, as corroborated by FTIR [21], was present along with the chemisorption process. In general, all the previously mentioned analysis results confirm the remarkable contribution of chemical adsorption throughout the CO_2 adsorption process in the nano-CaO adsorbent. One of the innovative aspects of this work was the favorable capacity of CO_2 capture in this adsorbent at moderate temperature and pressure.

In postcombustion processes from large stationary sources, the flow gas is released at temperatures in the range of 40–160°C and at a total pressure of approximately 1 atm [45]. The CO_2 capture behavior at moderate temperature and pressure using the prepared porous nano-CaO adsorbent is a feasible preprocess, which determined the intrinsic CO_2 capture capacity under typical postcombustion operating conditions. Furthermore, these results are of critical importance for carbon capture sequestration (CCS) technologies using adsorption processes.

3.6. Cyclic CO_2/nano-CaO adsorption-desorption

Cycling processes may be the cause of CaO-based adsorbent decay. Therefore, knowing the stability of the adsorbent is necessary for CCS technology implementation on a large scale. A high stability would result in the reduction of capital cost and energy. The q_{ad} of five cycles was 11.0 ± 0.1 meq/g; therefore, the adsorbent could be regenerated five times without any significant loss of CO_2 adsorption performance. Moreover, the material remains stable because the loss of the original samples after the five cycles was <2 wt%. Based on future energy scenarios, it is obvious that this porous nano-CaO adsorbent is an efficient material for balancing the costs and engineering feasibilities for different CO_2 capture processes. Previous experimental reports over multiple cycles of adsorption-desorption activity at different adsorption temperatures of CaO-based adsorbent showed a loss of carbonation activity with a high number of cycles [46].

4. Conclusions

The new porous nano-CaO adsorbent synthesized by chemical combustion/ball milling with im-

proved structural, chemical, and textural characteristics was able to absorb CO_2 with excellent CO_2 adsorption capacity at moderate temperatures. According to the Langmuir isotherms, this parameter increased from 9.48 mmol/g to 12.54 mmol/g when the temperature increased from 298 K to 323 K and to 348 K at ambient pressure. This achieved $CaCO_3$ formation on the porous nano-CaO adsorbent surface, which was accompanied by a very small fraction of physisorption. The adsorption of CO_2 could be adjusted finely to the kinetic pseudo-second-order and the intraparticle diffusion models, and this confirmed that the chemical process is carried out in gradual steps. The Langmuir adsorption isotherm was more accurate in predicting CO_2 adsorption on the porous CaO nanoadsorbent, which indicates monolayer coverage at the uniform surface adsorption sites characterized by chemisorption on a homogeneous material. The thermodynamic parameters showed that the positive sign of ΔH° in the studied temperature range indicated that the CO_2 adsorption reaction was endothermic and the magnitude revealed both physisorption and chemisorption processes. The positive value of ΔS° showed that the randomness at the solid-gas interface increased during the CO_2 adsorption process. The positive sign of the ΔG° values implies a nonspontaneous adsorption reaction, and the diminishing of the values with temperature suggests that the adsorption is favored at higher temperatures. The value of E_a is also in agreement with chemisorption as the adsorption mechanism. Five cycles of regeneration of the porous nano-CaO adsorbent did not cause any significant loss of performance or properties. Therefore, the nano-CaO adsorbent is a potential and efficient material to be applied for CO_2 capture in large-scale postcombustion CO_2 capture technologies. The obtained kinetic, equilibrium, and thermodynamic results provide valuable information for the design of improved adsorption schemes for CO_2 capture technologies at moderate temperatures using a new high-performance porous CaO nanoadsorbent.

Acknowledgements

The author is grateful to the National Institute of Nuclear Research (ININ), México, for financial support through projects CB-406 and CB-006, and the author also thanks I.Z. López-Malpica for her technical assistance.

References

[1] Granados-Correa F, Bonifacio-Martínez J, Hernández-Mendoza H, Bulbulian S. Capture of CO_2 on γ-Al_2O_3 materials prepared by solution-combustion and ball-milling processes. J Air Waste Manage Assoc. 2016;66:643–54.

[2] Azmi AA, Aziz MAA. Mesoporous adsorbent for CO_2 capture applications under mild condition: a review. J Environ Chem Eng. 2019;7:103022.

[3] Billo T, Shown I, Anbalagan AK, Effendi TA, Sabbah A, Fu F, et al. A mechanistic study of molecular CO_2 interaction and adsorption on carbon implanted SnS_2 thin film for photocatalytic CO_2 reduction activity. Nano Energy. 2020;72:104717.

[4] Gouveia LGT, Agustini CB, Perez-Lopez OW, Gutterres M. CO_2 adsorption using solids with different surface and acid-base properties. J Environ Chem Eng. 2020;8:103823.

[5] Huang CL, Wang PY, Li YY. Fabrication of electrospun CO_2 adsorption membrane for zinc-air battery application. Chem Eng J. 2020;395:125031.

[6] Garip M, Gizli N. Ionic liquid containing amine-based silica aerogels for CO_2 capture by fixed bed adsorption. J Molecular Liquids. 2020;310:113227.

[7] Sayari A, Belmabkhout Y, Serna-Guerrero R. Flue gas treatment via CO_2 adsorption. Chem Eng J. 2011;171:760–74.

[8] Choi S, Drese JH, Jones CW. Adsorbent materials for carbon dioxide capture from large anthropogenic point sources. ChemSusChem. 2009;2:796–854.

[9] Wang Q, Luo J, Zhong Z, Borgna A. CO_2 capture by solid adsorbents and their applications: current status and new trends. Energy Environ Sci. 2011;4:42–55.

[10] Romeo IM, Lara Y, Lisbona P, Martínez A. Economical assessment of comparative enhanced limestone for CO_2 capture cycles in powder plants. Fuel Process Technol. 2009;90:803–11.

[11] Zhang X, Liu W, Zhou S, Li Z, Sun J, Hu Y, et al. A review on granulation of CaO-based sorbent for carbon dioxide capture. Chem Eng J. 2022;446:136880.

[12] Khine EE, Koncz-Horvath D, Kristaly F, Ferenczi T, Karacs G, Baumli P, et al. Synthesis and characterization of calcium oxide nanoparticles for CO_2 capture. J Nanoparticle Res. 2022;24:139.

[13] Sun H, Wang J, Liu X, Shen B, Parlett CMA, Adwek G, et al. Fundamental studies of carbon capture using CaO-based materials. J Mater Chem A. 2019;7:9977–87.

[14] Sun H, Wu C, Shen B, Zhang X, Zhang Y, Huang J. Progress in the development and application of CaO-based adsorbents for CO_2 capture – A review. Mater Today Sustain. 2018;1–2:1–27.

[15] Zhao B, Ma L, Shi H, Liu K, Zhang J. Calcium precursor from stirring processes at room temperature for controllable preparation of nano-structure CaO sor-

bents for high-temperature CO_2 adsorption. J CO_2 Util. 2018;25:315–22.

[16] Ammendola P, Raganati F, Chirone R. CO_2 adsorption on a fine activated carbon in a sound assisted fluidized bed. Thermodynamics and kinetics. Chem Eng J. 2017;322:302–13.

[17] Kavosh M, Patchigolla K, Oakey JE, Anthony EJ, Champagne SR, Hughes R. Pressurized calcination-atmospheric carbonation of limestone for cyclic CO_2 capture from flue gases. Chem Eng Res Des. 2015;102:116–23.

[18] Shan L, Li H, Meng B, Meng J, Yu Y, Min Y. Improvement of CO_2 capture performance of calcium-based adsorbent modified with palygorskite. Chinese J Chem Eng. 2016;24:1283–9.

[19] Baxter J, Bianz Z, Chen C, Danielson D, Dresselhaus MS, Fedorov AG. Nanoscale design to enable the revolution in renewable energy. Energy Environ Sci. 2009;2:559–88.

[20] Liang G, Hout J, Schultz R. Hydrogen storage properties of the mechanically alloyed $LaNi_5$-based materials. J Alloys Compd. 2011;320:133–9.

[21] Granados-Pichardo A, Granados-Correa F, Sánchez-Mendieta V, Hernández-Mendoza H. New CaO-based adsorbents prepared by solution combustion and high-energy ball-milling processes for CO_2 adsorption: textural and structural influences. Arab J Chem. 2020;13:171–83.

[22] Pontiga F, Valverde JM, Moreno H, Duran-Olivencia FJ. Dry gas-solid carbonation in fluidized beds of $Ca(OH)_2$ and nanosilica/$Ca(OH)_2$ at ambient temperature and low CO_2 pressure. Chem Eng J. 2013;222:546–52.

[23] Rashidi A, Yusupa S, Loong LH. Kinetic studies on carbon dioxide capture activity using activated carbon. Chem Eng Trans. 2013;35:361–6.

[24] Patil KS, Aruna ST, Mimami T. Combustion synthesis: an update. Curr Opin Solid State Mater Sci. 2002;6:507–12.

[25] Granados-Correa F, Bulbulian S. Co(II) adsorption in aqueous media by a synthetic Fe-Mn binary oxide adsorbent. Water Air Soil Pollut. 2012;223:4089–100.

[26] Ho YS, McKay G. The kinetics of sorption of divalent metal ions onto sphagnum moss peat. Water Res. 2000;34:735–42.

[27] Ho YS, McKay G. Pseudo-second order model for sorption processes. Process Biochem. 1999;34:452–65.

[28] Liu Y, Liu YJ. Review-biosorption isotherms, kinetics and thermodynamics. Sep Purif Technol. 2008;61:229–42.

[29] Song G, Zhu X, Chen R, Liao Q, Ding Y, Chen L. An investigation of CO_2 adsorption kinetics on porous magnesium oxide. Chem Eng J. 2016;283:175–83.

[30] Foo KY, Hameed BH. Review-insights into the modelling of adsorption isotherm systems. Chem Eng J. 2010;156:2–10.

[31] Kumar KV, Optimum sorption isotherm by linear and non-linear methods for malachite green onto lemon peel. Dyes Pigm. 2007;74:595–7.

[32] Jeong-Hak C, Chang-Han L. Evaluation of Sr and Cs ions adsorption capacities with zeolitic materials synthesized from various mass ratios of NaOH to coal fly ash. Environ Eng Res. 2022;27:200662.

[33] Guyo U, Mhonyera J, Moyo M. Pb(II) adsorption from aqueous solutions by raw and treated biomass of maize stover – A comparative study. Process Saf Environ Prot. 2015;93:192–200.

[34] Helfferich F. Ion exchange. New York: McGraw-Hill; 1964.

[35] Moroto-Valer MM, Tang Z, Zhang Y. CO_2 capture by activated and impregnated anthracites. Fuel Process Technol. 2005;86:1487–502.

[36] Pighini C, Belin T, Mijoin J, Magnoux P, Costentin G, Lauron-Pernot H. Microcalorimetric and thermodynamic studies of CO_2 and methanol adsorption on magnesium oxide. Appl Surf Sci. 2011;257:6952–62.

[37] Aksu Z. Determination of the equilibrium, kinetic and thermodynamic parameters of the batch biosorption of nickel(II) ions onto Chlorella vulgaris. Process Biochem. 2002;38:89–99.

[38] Tran HN, You SJ, Chao HP. Thermodynamic parameters of cadmium adsorption onto orange peel calculated from various methods: a comparison study. J Environ Chem. 2016;4:2671–82.

[39] Seker A, Shahwan T, Eroglu AE, Yilmaz S, Demirel Z, Dalay C. Equilibrium, thermodynamic and kinetic studies for the biosorption of aqueous lead(II), cadmium(II) and nickel(II) ions on Spirulina platensis. J Hazard Mater. 2008;154:973–80.

[40] Khoshandam B, Kumar RV, Allahgholi I. Mathematical modeling of CO_2 removal using carbonation with CaO: the grain model. Korean J Chem Eng. 2010;27:766–76.

[41] Gutiérrez-Bonilla E, Granados-Correa F, Sánchez-Mendieta V, Morales-Luckie RA. MgO-based adsorbents for CO_2 adsorption: influence of structural and textural properties on the CO_2 adsorption performance. J Environ Sci. 2017;57:418–28.

[42] Valverde JM, Sanchez-Jimenez PE, Perez-Maqueda LA, Quintanilla MAS, Perez-Vaquero J. Role of crystal structure on CO_2 capture by limestone derived CaO subjected to carbonation/recarbonation/calcination cycles at Ca-looping conditions. Appl Energy. 2014;125:264–75.

[43] Fennell PS, Pacciani R, Dennis JS, Davidson JF, Hayhurst AN. The effects of repeated cycles of calcination and carbonation on a variety of different limestones, as measured in a hot fluidized bed of sand. Energy Fuels. 2007;21:2072–81.

[44] Lee SY, Park SJ. Preparation and characterization of ordered porous carbons for increasing hydrogen storage behaviours. J Solid State Chem. 2011;184:2655–60.

[45] Kaithwas A, Prasad M, Kulshreshtha A, Verna S. Industrial wastes derived solid adsorbents for CO_2 capture: a mini review. Chem Eng Res Des. 2012;90:1632–41.

[46] Chen H, Zhao C. Development of a CaO based sorbent with improved cyclic stability for CO_2 capture in pres-

surized carbonation. Chem Eng J. 2011;171:197–205.

Received 2022-07-01
Accepted 2022-09-03